

Magnetoresistance oscillations in two-dimensional electron systems under monochromatic and bichromatic radiations

X. L. Lei and S. Y. Liu

Department of Physics, Shanghai Jiaotong University, 1954 Huashan Road, Shanghai 200030, China

The magnetoresistance oscillations in high-mobility two-dimensional electron systems induced by two radiation fields of frequency 31 GHz and 47 GHz, are analyzed in a wide magnetic-field range down to 100 G, using the balance-equation approach to magnetotransport for high-carrier-density systems. The frequency mixing processes are shown to be important. The predicted peak positions, relative heights, radiation-intensity dependence and their relation with monochromatic resistivities, are in good agreement with recent experimental finding [Zudov *et al.* Phys. Rev. Lett. **96**, 236804 (2006)].

PACS numbers: 73.50.Jt, 73.40.-c, 78.67.-n, 78.20.Ls

The fascinating phenomena of radiation-induced magnetoresistance oscillations (RIMOs) and zero-resistance states (ZRS) in high mobility two-dimensional (2D) electron systems,^{1,2,3,4,5} continue to attract much experimental^{6,7,8,9,10,11,12,13,14,15,16,17} and theoretical^{18,19,20,21,22,23,24,25,26,27,28,29,30,31,32,33} attention.

Under the influence of a monochromatic microwave radiation of frequency $\omega/2\pi$, the low-temperature magnetoresistance of a 2D electron gas (EG), exhibits periodic oscillation as a function of the inverse magnetic field $1/B$. The oscillation features the periodical appearance of peak-valley pairs around node points $\omega/\omega_c = j$ ($j = 1, 2, 3, 4, \dots$, $\omega_c = eB/m$ is the cyclotron frequency). With increasing the radiation intensity the oscillation amplitude increases and the measured resistance around the minima of a few lowest- j pairs can drop down to zero. The nature of this observed ZRS, which was considered as the result of absolute negative resistance,¹⁸ remains an issue for experimental confirmation. A recent measurement of photoresistance under simultaneous illumination of two radiation fields of different frequencies by Zudov *et al.*¹⁶ provided a plausible evidence to link the ZRS to the negative resistance. However, the empirical superposition relation between the bichromatic and two monochromatic resistances, needs refinement and justification.¹⁶ A convincing theoretical treatment capable of reproducing the experimental results through the whole magnetic field range is highly desirable. In this paper we present such an examination of bichromatic-radiation induced photoresistance based on the balance-equation approach³⁴ to magnetotransport for high-carrier-density systems.

In this balance-equation theory of photon-assisted scattering,^{21,29} the transport state of a 2DEG subject to a dc field \mathbf{E}_0 and a normally incident monochromatic radiation $\mathbf{E}_i = \mathbf{E}_{is} \sin(\omega t) + \mathbf{E}_{ic} \cos(\omega t)$, is described by the electron drift velocity $\mathbf{v}_0 + \mathbf{v}_c \cos(\omega t) + \mathbf{v}_s \sin(\omega t)$ and the electron temperature T_e . They are determined by the balance equations (8)–(11) in Ref. 29. The linear

$(\mathbf{v}_0 \rightarrow 0)$ magnetoresistivity is expressed as

$$R_{xx}^\omega(\xi) = -\frac{1}{N_e^2 e^2} \sum_{\mathbf{q}_\parallel} q_x^2 |U(\mathbf{q}_\parallel)|^2 \sum_{n=-\infty}^{\infty} J_n^2(\xi) \Pi'_2(\mathbf{q}_\parallel, n\omega), \quad (1)$$

where $\mathbf{q}_\parallel \equiv (q_x, q_y)$, N_e is the electron density, $U(\mathbf{q}_\parallel)$ is the impurity potential, $\xi \equiv \sqrt{(\mathbf{q}_\parallel \cdot \mathbf{v}_c)^2 + (\mathbf{q}_\parallel \cdot \mathbf{v}_s)^2}/\omega$, and $\Pi'_2(\mathbf{q}_\parallel, \Omega) \equiv \frac{\partial}{\partial \Omega} \Pi_2(\mathbf{q}_\parallel, \Omega)$ stands for the differentiation of the imaginary part of the electron density correlation function with respect to its frequency variable.

The $\Pi_2(\mathbf{q}_\parallel, \Omega)$ function of a 2D system in a magnetic field can be expressed as sums over all Landau levels:

$$\Pi_2(\mathbf{q}_\parallel, \Omega) = \frac{1}{2\pi l_B^2} \sum_{l, l'} C_{l, l'} (l_B^2 q_\parallel^2/2) \Pi_2(l, l', \Omega), \quad (2)$$

$$\Pi_2(l, l', \Omega) = -\frac{2}{\pi} \int d\varepsilon [f(\varepsilon) - f(\varepsilon + \Omega)] \times \text{Im}G_l(\varepsilon + \Omega) \text{Im}G_{l'}(\varepsilon), \quad (3)$$

where $C_{l, l+m}(Y) \equiv l![(l+m)!]^{-1} Y^m e^{-Y} [L_l^m(Y)]^2$ with $L_l^m(Y)$ the associate Laguerre polynomial, $l_B \equiv \sqrt{1/|eB|}$ is the magnetic length, $f(\varepsilon) = \{\exp[(\varepsilon - \mu)/T_e] + 1\}^{-1}$ is the Fermi distribution function at electron temperature T_e . The density-of-states (DOS) of the l -th Landau level is modeled with a Gaussian form, $\text{Im}G_l(\varepsilon) = -(\sqrt{2\pi}/\Gamma) \exp[-2(\varepsilon - \varepsilon_l)^2/\Gamma^2]$, having a half-width $\Gamma = (8\omega_c \alpha / \pi m \mu_0)^{1/2}$ around the level center $\varepsilon_l = l\omega_c$. Here m is the carrier effective mass, μ_0 is the linear mobility at lattice temperature T in the absence of the magnetic field, and α is a semiempirical parameter to take account of the difference of the transport scattering time determining the mobility μ_0 , from the single particle lifetime related to Landau level broadening.²⁹

It can be seen from the expressions (2) and (3) that, *in the case of low electron temperature ($T_e \ll \epsilon_F$, the Fermi level) and large Landau-level filling factor ν , for any integer N satisfying $|N| \ll \nu$, $\Pi'_2(\mathbf{q}_\parallel, \Omega + N\omega_c) = \Pi'_2(\mathbf{q}_\parallel, \Omega)$.* Thus, when $\omega = l\omega_c$ ($l = 1, 2, \dots$), the $\Pi'_2(\mathbf{q}_\parallel, n\omega)$ function in (1) is independent of n , that

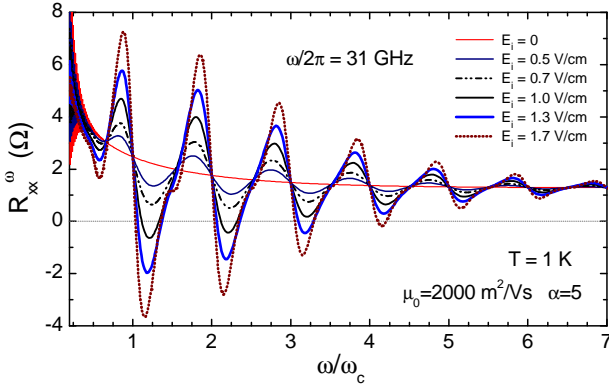


FIG. 1: (Color online) The magnetoresistivity R_{xx}^{ω} induced by monochromatic radiations of frequency $\omega/2\pi = 31$ GHz at lattice temperature $T = 1$ K, in a GaAs-based 2DEG with $N_e = 2.4 \times 10^{15} \text{ m}^{-2}$, $\mu_0 = 2000 \text{ m}^2/\text{Vs}$ and $\alpha = 5$.

$\sum_n J_n^2(\xi) \Pi'_2(\mathbf{q}_{\parallel}, n\omega) = \Pi'_2(\mathbf{q}_{\parallel}, 0)$, and

$$R_{xx}^{\omega}(\xi) = -\frac{1}{N_e^2 e^2} \sum_{\mathbf{q}_{\parallel}} q_x^2 |U(\mathbf{q}_{\parallel})|^2 \Pi'_2(\mathbf{q}_{\parallel}, 0). \quad (4)$$

(4) indicates that at cyclotron frequency and its harmonics, $\omega = l\omega_c$ ($l = 1, 2, \dots$), the difference of $R_{xx}^{\omega}(\xi)$ driven by monochromatic frequency- ω fields of different strengths, can appear only through the difference of electron heating contained in the Π_2 function.³⁵ Under the condition of $T_e \ll \epsilon_F$, the effect of electron heating on photoresistance is quite weak,²¹ therefore, at integer- ω_c value of frequency ω , the magnetoresistivity with radiation is essentially the same as that without radiation, $R_{xx}^{\omega}(\xi) \simeq R_{xx}(0)$, or *the photoresponse vanishes at cyclotron resonance and its harmonics*.

This is clearly seen in Fig. 1, where we plot the calculated magnetoresistivity R_{xx}^{ω} of a GaAs-based 2DEG with $N_e = 2.4 \times 10^{15} \text{ m}^{-2}$, $\mu_0 = 2000 \text{ m}^2/\text{Vs}$ and $\alpha = 5$, irradiated by linearly polarized monochromatic waves of frequency $\omega/2\pi = 31$ GHz having incident amplitudes $E_i = 0, 0.5, 0.7, 1.0, 1.3$ and 1.7 V/cm at lattice temperature $T = 1 \text{ K}$. The scattering is assumed due to short-range impurities and the material parameters used are the same as in Ref. 33. All the curves, with and without radiation, cross at $\omega/\omega_c = 1, 2, 3, 4, 5, 6$ and 7 . This feature, being pointed out before theoretically,^{19,20,21,22} has been confirmed by experiments.^{4,5,8,10} It is quite general, independent of the polarization state of the radiation, the behavior of the elastic scattering, and other properties of 2DEG, and holds quite precisely up to rather strong radiation field even multiphoton processes play important role, as long as the the 2DEG remains in degenerate ($T_e \ll \epsilon_F$). It thus provides a convenient and accurate method to determine the effective mass of 2DEG.

Another feature which shows up when the radiation strength is modest that contributions from two- and higher photon processes are negligible and MIROs result

mainly from single-photon-assisted processes:

$$R_{xx}^{\omega}(\xi) \simeq -\frac{1}{N_e^2 e^2} \sum_{\mathbf{q}_{\parallel}} q_x^2 |U(\mathbf{q}_{\parallel})|^2 [J_0^2(\xi) \Pi'_2(\mathbf{q}_{\parallel}, 0) + J_1^2(\xi) \Pi'_2(\mathbf{q}_{\parallel}, \omega) + J_{-1}^2(\xi) \Pi'_2(\mathbf{q}_{\parallel}, -\omega)]. \quad (5)$$

Since the DOS function decays rapidly when deviating from the center of each Landau level, the magnitude of $\Pi'_2(\mathbf{q}_{\parallel}, \omega)$ reaches a minimum of almost zero when $\omega/\omega_c = (l + \frac{1}{2})$ ($l = 1, 2, 3, \dots$). Therefore around these half-integer- ω_c positions, the magnetoresistivity

$$R_{xx}^{\omega}(\xi) \simeq -\frac{1}{N_e^2 e^2} \sum_{\mathbf{q}_{\parallel}} q_x^2 |U(\mathbf{q}_{\parallel})|^2 J_0^2(\xi) \Pi'_2(\mathbf{q}_{\parallel}, 0) \quad (6)$$

is only weakly dependent on radiation strength through $J_0^2(\xi)$, i.e. half-integer- ω_c positions are approximately node points for modest radiation. This can also be seen in Fig. 1 where almost all the resistivity curves cross at $\omega/\omega_c = 3.5, 4.5, 5.5$ and 6.5 , and the curves of lower radiation strengths cross at $\omega/\omega_c = 1.5$ and 2.5 .

Under normally illuminating bichromatic radiation $\mathbf{E}_{i1} = \mathbf{E}_{i1s} \sin(\omega_1 t) + \mathbf{E}_{i1c} \cos(\omega_1 t)$ and $\mathbf{E}_{i2} = \mathbf{E}_{i2s} \sin(\omega_2 t) + \mathbf{E}_{i2c} \cos(\omega_2 t)$, the transport state of a 2DEG can be described by the electron drift velocity oscillating at both base radiation frequencies, $\mathbf{v}_0 + \mathbf{v}_{1c} \cos(\omega_1 t) + \mathbf{v}_{1s} \sin(\omega_1 t) + \mathbf{v}_{2c} \cos(\omega_2 t) + \mathbf{v}_{2s} \sin(\omega_2 t)$, together with the electron temperature T_e . They are determined by the balance equations (5)–(10) in Ref. 33. The linear ($\mathbf{v}_0 \rightarrow 0$) magnetoresistivity is expressed as

$$R_{xx}^{\omega_1 \omega_2}(\xi_1, \xi_2) = -\frac{1}{N_e^2 e^2} \sum_{\mathbf{q}_{\parallel}} q_x^2 |U(\mathbf{q}_{\parallel})|^2 \times \sum_{n_1, n_2 = -\infty}^{\infty} J_{n_1}^2(\xi_1) J_{n_2}^2(\xi_2) \Pi'_2(\mathbf{q}_{\parallel}, n_1 \omega_1 + n_2 \omega_2). \quad (7)$$

where $\xi_1 \equiv \sqrt{(\mathbf{q}_{\parallel} \cdot \mathbf{v}_{1c})^2 + (\mathbf{q}_{\parallel} \cdot \mathbf{v}_{1s})^2}/\omega_1$ and $\xi_2 \equiv \sqrt{(\mathbf{q}_{\parallel} \cdot \mathbf{v}_{2c})^2 + (\mathbf{q}_{\parallel} \cdot \mathbf{v}_{2s})^2}/\omega_2$. (7) indicates that bichromatic $R_{xx}^{\omega_1 \omega_2}$ contains, besides the weighted superposition of mono- ω_1 and mono- ω_2 contributions, $J_0^2(\xi_1) R_{xx}^{\omega_2}(\xi_2) + J_0^2(\xi_2) R_{xx}^{\omega_1}(\xi_1)$, also mixing ω_1 and ω_2 contributions (term with $n_1 = n_2 = 0$ and terms with both $n_1, n_2 \neq 0$).

It is easy seen that, in the degenerate and large- ν case, at positions $\omega_2 = l\omega_c$ ($l = 1, 2, 3, \dots$), the $\Pi'_2(\mathbf{q}_{\parallel}, n_1 \omega_1 + n_2 \omega_2)$ function in (7) does not depend on n_2 , thus

$$R_{xx}^{\omega_1 \omega_2}(\xi_1, \xi_2) = -\frac{1}{N_e^2 e^2} \sum_{\mathbf{q}_{\parallel}} q_x^2 |U(\mathbf{q}_{\parallel})|^2 \times \sum_{n_1 = -\infty}^{\infty} J_{n_1}^2(\xi_1) \Pi'_2(\mathbf{q}_{\parallel}, n_1 \omega_1) \approx R_{xx}^{\omega_1}(\xi_1), \quad (8)$$

equals the monochromatic resistivity under ω_1 - \mathbf{E}_{i1} radiation (effect of electron temperature difference on photoresistance is negligible). This means that all the bichromatic $R_{xx}^{\omega_1 \omega_2}(\xi_1, \xi_2)$ curves with fixed \mathbf{E}_{i1} but changing

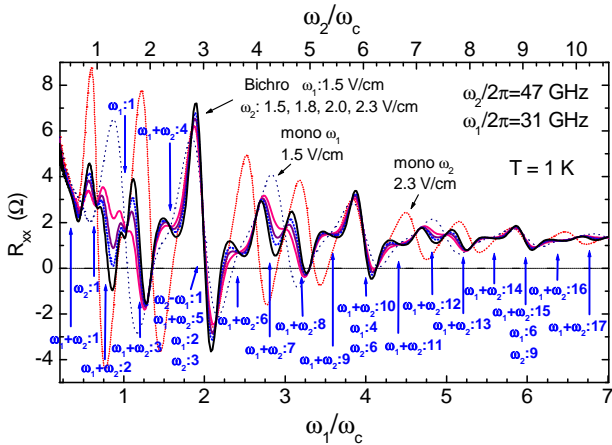


FIG. 2: (Color online) The magnetoresistivity R_{xx} induced by bichromatic or monochromatic radiations ($R_{xx}^{\omega_1\omega_2}$, $R_{xx}^{\omega_1}$ or $R_{xx}^{\omega_2}$) in the same 2DEG as described in Fig. 1.

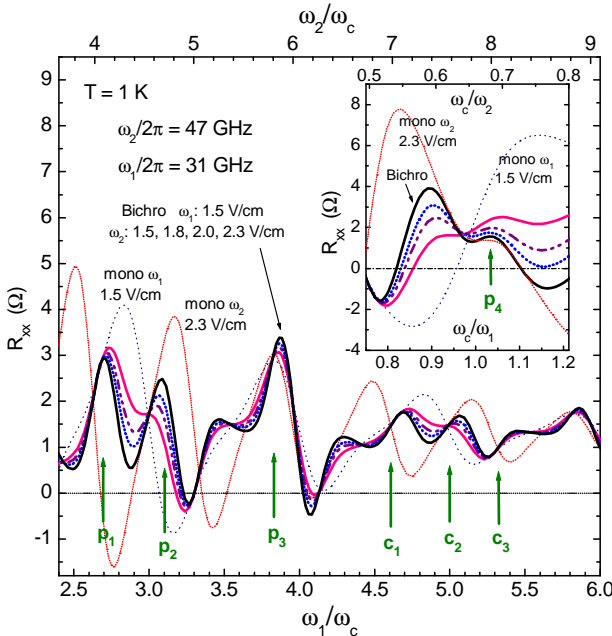


FIG. 3: (Color online) Same as figure 2 in an enlarged scale.

E_{i2} , cross with the monochromatic $R_{xx}^{\omega_1}(\xi_1)$ curve of E_{i1} at integer- ω_c points of ω_2 .

Likewise, at integer- ω_c points of ω_1 ,

$$R_{xx}^{\omega_1\omega_2}(\xi_1, \xi_2) \approx R_{xx}^{\omega_2}(\xi_2). \quad (9)$$

In the case of $\omega_2 \sim 1.5\omega_1$, even and odd ω_c points exhibit somewhat different behavior. At an even- ω_c point of ω_1 ($\omega_1 = 2\omega_c, 4\omega_c$ or $6\omega_c$), ω_2 also closes to an integer ω_c ($\omega_2 \approx 3\omega_c, 6\omega_c$ and $9\omega_c$) that $R_{xx}^{\omega_1\omega_2}(\xi_2)$ is almost identical to the dark resistivity $R_{xx}(0)$, independent of E_{i2} . Therefore, all bichro-resistivity $R_{xx}^{\omega_1\omega_2}$, mono-resistivity $R_{xx}^{\omega_1}$ and mono-resistivity $R_{xx}^{\omega_2}$, cross at these

points with dark resistivity $R_{xx}(0)$. At an odd- ω_c point of ω_1 ($\omega_1 = \omega_c, 3\omega_c, 5\omega_c$ or $7\omega_c$), ω_2 closes to a half-integer ω_c ($\omega_2 \approx 1.5\omega_c, 4.5\omega_c, 7.5\omega_c$ or $10.5\omega_c$). It is a node point of $R_{xx}^{\omega_2}(\xi_2)$ when E_{i2} changes modestly. Thus, at these points bichromatic $R_{xx}^{\omega_1\omega_2}$ and monochromatic $R_{xx}^{\omega_1}$ and $R_{xx}^{\omega_2}$ are nearly the same, but may be somewhat different from the dark resistivity.

Figure 2 demonstrates the calculated magnetoresistivity $R_{xx}^{\omega_1\omega_2}$ versus the inverse magnetic field for the same GaAs-based 2D system as described in Fig. 1 under linearly polarized bichromatic radiation of $\omega_1/2\pi = 31$ GHz and $\omega_2/2\pi = 47$ GHz with incident amplitudes $E_{i1} = 1.5$ V/cm and $E_{i2} = 1.5, 1.8, 2.0$, and 2.3 V/cm at $T = 1$ K. The monochromatic $R_{xx}^{\omega_1}$ at $E_{i1} = 1.5$ V/cm and $R_{xx}^{\omega_2}$ at $E_{i2} = 2.3$ V/cm are also shown. Comparing with the monochromatic ones, the bichromatic curve consists of much more sizable peak-valley pairs. Since only minor high-order structures showing up in both monochromatic curves at these radiation strengths, most of the pairs appearing in the bichromatic curves relate to mixing photon processes. We have identified the lowest order ($|n_1| \leq 1$ and $|n_2| \leq 1$) individual (ω_1 or ω_2) and mixing ($\omega_1 - \omega_2$ or $\omega_1 + \omega_2$) photon-assisted electron transition processes to all the pairs in the figure. Except those pairs around $\omega_2/\omega_c = 1$ and $\omega_1/\omega_c = 1$, which relate to single- ω_2 and single- ω_1 processes, and those around $\omega_1/\omega_c = 2, 4$ and 6 , which relate to both individual and mixing photon processes $\omega_1 + \omega_2 : l$ with electron transitions jumping l Landau-level spacings.³³

A lower magnetic-field portion of this figure is redrawn in Fig. 3 with enlarged scale for clearer comparison with experiments. The predicted positions and relative heights of bichromatic peaks p_1, p_2 and p_3 around $\omega_1/\omega_c = 2.7, 3.1$ and 3.9 , and the predicted approximate crossing points c_1 (at $\omega_2/\omega_c = 7$), c_2 (at $\omega_1/\omega_c = 5$) and c_3 (at $\omega_2/\omega_c = 8$), well reproduce³⁶ the experimental bichromatic peaks around 270, 222 and 182 G and the experimental crossing points marked in Fig. 2 of Ref. 16, where the empirical superposition relation is considered valid. The portion of $\omega_c/\omega_1 = 1$ vicinity of Fig. 2 is also replotted in the inset of Fig. 3 as functions of B . A bichromatic peak p_4 shows up clearly around $\omega_c/\omega_1 = 1.03$, where mono- ω_1 curve has a large positive value and mono- ω_2 curve exhibits a small positive peak. This is exactly what observed experimentally around $B \approx 730$ G, where the superposition relation is apparently invalid.¹⁶ The present theory, instead, is able to provide a unified description for the bichromatic resistivity and its relation to individual monochromatic ones over the wide magnetic field range.

This work was supported by Projects of the National Science Foundation of China and the Shanghai Municipal Commission of Science and Technology.

¹ V. I. Ryzhii, Sov. Phys. Solid State **11**, 2087 (1970).

² M. A. Zudov, R. R. Du, J. A. Simmons, and J. R. Reno, Phys. Rev. B **64**, 201311(R) (2001).

³ P. D. Ye, L. W. Engel, D. C. Tsui, J. A. Simmons, J. R. Wendt, G. A. Vawter, and J. L. Reno, Appl. Phys. Lett. **79**, 2193 (2001).

⁴ R. G. Mani, J. H. Smet, K. von Klitzing, V. Narayananmurti, W. B. Johnson, and V. Umansky, Nature **420**, 646 (2002).

⁵ M. A. Zudov, R. R. Du, L. N. Pfeiffer, and K. W. West, Phys. Rev. Lett. **90**, 046807 (2003).

⁶ C. L. Yang, M. A. Zudov, T. A. Knuutila, R. R. Du, L. N. Pfeiffer, and K. W. West, Phys. Rev. Lett. **91**, 096803 (2003).

⁷ S. I. Dorozhkin, JETP Lett. **77**, 577 (2003).

⁸ R. G. Mani, J. H. Smet, K. von Klitzing, V. Narayananmurti, W. B. Johnson, and V. Umansky, Phys. Rev. Lett. **92**, 146801 (2004).

⁹ R. L. Willett, L. N. Pfeiffer, and K. W. West, Phys. Rev. Lett. **93**, 026804 (2004).

¹⁰ R. G. Mani, Physica E **25**, 189 (2004); Appl. Phys. Lett. **85**, 4962 (2004).

¹¹ M. A. Zudov, Phys. Rev. B **69**, 041304(R) (2004).

¹² S. A. Studenikin, M. Potenski, A. Sachrajda, M. Hilke, L. N. Pfeiffer, and K. W. West, IEEE Tran. on Nanotech. **4**, 124 (2005).

¹³ S. I. Dorozhkin, J. H. Smet, V. Umansky, K. von Klitzing, Phys. Rev. B **71**, 201306(R) (2005).

¹⁴ R. G. Mani, Phys. Rev. B, **72**, 075327 (2005).

¹⁵ J. H. Smet, B. Gorshunov, C. Jiang, L. Pfeiffer, K. West, V. Umansky, M. Dressel, R. Meisels, F. Kuchar, and K. von Klitzing, Phys. Rev. Lett. (2005).

¹⁶ M. A. Zudov, R. R. Du, L. N. Pfeiffer, and K. W. West, Phys. Rev. Lett. **96**, 236804 (2006).

¹⁷ M. A. Zudov, R. R. Du, L. N. Pfeiffer, and K. W. West, Phys. Rev. B **73**, 041303(R) (2006).

¹⁸ A. V. Andreev, I. L. Aleiner, and A. J. Millis, Phys. Rev. Lett. **91**, 056803 (2003).

¹⁹ A. C. Durst, S. Sachdev, N. Read, and S. M. Girvin, Phys. Rev. Lett. **91**, 086803 (2003).

²⁰ J. Shi and X. C. Xie, Phys. Rev. Lett. **91**, 086801 (2003).

²¹ X. L. Lei and S. Y. Liu, Phys. Rev. Lett. **91**, 226805 (2003); X. L. Lei, J. Phys.: Condens. Matter **16**, 4045 (2004).

²² V. Ryzhii and R. Suris, J. Phys.: Condens. Matter **15**, 6855 (2003).

²³ M. G. Vavilov and I. L. Aleiner, Phys. Rev. B **69**, 035303 (2004).

²⁴ S. A. Mikhailov, Phys. Rev. B **70**, 165311 (2004).

²⁵ J. Dietel, L. I. Glazman, F. W. J. Hekking, F. von Oppen, Phys. Rev. B **71**, 045329 (2005).

²⁶ M. Torres and A. Kunold, Phys. Rev. B **71**, 115313 (2005).

²⁷ I. A. Dmitriev, M. G. Vavilov, I. L. Aleiner, A. D. Mirlin, and D. G. Polyakov, Phys. Rev. B **71**, 115316 (2005).

²⁸ J. Iñarrea and G. Platero, Phys. Rev. Lett. **94**, 016806 (2005); Phys. Rev. B **72**, 193414 (2005).

²⁹ X. L. Lei and S. Y. Liu, Phys. Rev. B **72**, 075345 (2005); Appl. Phys. Lett. **86**, 262101 (2005); **88**, 212109 (2006).

³⁰ V. Ryzhii, Jpn. J. Appl. Phys., Part 1 **44**, 6600 (2005).

³¹ C. Joas, J. Dietel, and F. von Oppen, Phys. Rev. B **72**, 165323 (2005).

³² T. K. Ng and Lixin Dai, Phys. Rev. B **72**, 235333 (2005).

³³ X. L. Lei, Phys. Rev. B **73**, 235322 (2006).

³⁴ X. L. Lei and C. S. Ting, Phys. Rev. B **32**, 1112 (1985); X. L. Lei, J. Appl. Phys. **84**, 1396 (1998); S. Y. Liu and X. L. Lei, J. Phys.: Condens. Matter **15**, 4411 (2003).

³⁵ This conclusion is in contrast with that of high temperature and low Landau-level filling case, where the direct photon-assisted scattering, rather than the electron heating, was shown to be the dominant mechanism for the photoresponse at cyclotron resonance. See, e.g. X. L. Lei and S.Y. Liu, Appl. Phys. Lett. **82**, 3904 (2003).

³⁶ If $\omega_c/\omega_1 = 1.03$ is considered at 730 G, the p_1 , p_2 and p_3 locate respectively at 263, 229 and 182 G.